JOURNAL OF COMPUTATIONAL PHYSICS **144,** 1–16 (1998)
ARTICLE NO. CP985992

Development of a High-Resolution Scheme for a Multi-dimensional Advection-Diffusion Equation

Tony W. H. Sheu, S. K. Wang, and S. F. Tsai

Department of Naval Architecture and Ocean Engineering, National Taiwan University, 73 Chou-Shan Road, Taipei, Taiwan, Republic of China
E-mail: sheu@indy.na.ntu.edu.tw

Received April 14, 1997; revised March 24, 1998

In this article, we present a composite scheme to solve the scalar transport equation in a two-dimensional space. The aim of this study is to accurately resolve sharp profiles in the flow. The theory of the M-matrix serves as the theoretical foundation for achieving this goal. Attempts to extend the approach to resolve discontinuities in all cases motivate the development of the composite scheme. For this study, a conditionally monotonic Legendre polynomial finite element model is used together with an unconditionally monotonic scheme. Computational evidence reveals that the composite model improves stability while it maintains accuracy. The application scope is thus greatly extended.

1. INTRODUCTION

Attempts to understand the nature of the discretization scheme for Navier–Stokes equations could be considered as a first step towards a successful application of numerical methods to practical flow simulations. However, Navier–Stokes equations are too complex for researchers to conduct an in-depth fundamental analysis. As a result, the advective-diffusive scalar equation, regarded as the simplest prototype equation capable of characterizing these equations, is examined as a linear, steady-state model for Navier–Stokes equations in the development of finite elements for problems in fluid dynamics. Detailed investigation of this model equation is also preferable because it is amenable to analytic solution, thus facilitating comparison studies conducted on discretization equations. The foregoing explains why this model equation has been extensively studied for several years.

For convection-dominated problems, use of center-based schemes such as the Galerkin formulation may result in spurious oscillations, which in turn causes severe loss of accuracy and stability. For this reason efforts were dedicated to suppressing these wiggles for the case

0021-9991/98 $25.00

of prevailing convection type. Besides numerical stability, solution accuracy, computational efficiency, and case of programming are also viewed as being crucial factors in the development of an effective scheme. Retaining the scheme stability without sacrificing solution accuracy motivates the present development of an advection-diffusion finite element model in two dimensions.

In the presence of discontinuities, discretization schemes developed for solving convection-dominated problems have been mostly based on the total variation diminishing (TVD) underlying concept [1]. While TVD schemes give good local suppression of high-frequency oscillations near jumps, the lack of a multi-dimensional TVD constraint condition forbids the extension to analyses involving spatial dimensions more than one. Different bounded flux discretization schemes emerged accordingly. To the best of the authors' knowledge, the flux corrected transport (FCT) algorithm of Boris and Book [2], which was later generalized by Zalesak [3], is known as the first multi-dimensional high-resolution scheme so far devised. Readers are referred to Woodward and Colella [4] who gave a thorough survey of multi-dimensional discontinuity-capturing schemes.

We review recently developed schemes in the context of the linear scalar multi-dimensional equation for pure advection and the scalar equation with advection and diffusion. The Filter Remedy and Methodology (FRAM) of Chapman [5] and the scheme constructed through use of flux limiters [6] have been applied to flow equations by one of the present authors [7]. Among other schemes, the Simple High-Accuracy Resolution Program (SHARP) [8] and Non-oscillatory Integrally Reconstructed Volume-Averaged Numerical Advection (NIRVANA) scheme, developed by Leonard *et al.* [9, 10], and SMART (Sharp and Monotonic Algorithm for Realistic Transport), developed by Gaskell and Lau [11], have also gained wide popularity. More recently, the FCT algorithm has been used together with the Taylor–Galerkin finite element framework to resolve sharp profiles [12–15]. Deconinck *et al.* [16] has presented a class of truly multi-dimensional upwind schemes on unstructured cell-vertex grids. These schemes are featured by their compact stencils and are known to produce sharp resolution of discontinuities with no overshoots. In 1988, Galeão and Carmo [17] proposed a consistent approximate upwind Petrov–Galerkin formulation for convection-diffusion problems. Spurious oscillations can be well suppressed by means of a discontinuity-capturing term added to the SUPG (Streamline Upwind Petrov-Galerkin) method of Brooks and Hughes [18]. This discontinuity-capturing term also provides an extra control over derivatives in the gradient direction.

The other class of approaches to construct oscillation-free solutions is to apply a global positivity principle to explicit schemes [19, 20]. While the positivity principle has a sound theoretical foundation and is easy to be implemented in existing computer codes, its scope of application is limited to explicit schemes. Filtering techniques applicable to analyses involving solving field variables from a simultaneous set of algebraic equations must be devised. To avoid erroneous oscillations near jumps, refinements on test functions have been made by Sheu *et al.* [21] who modified the SUPG model [18]. This modification helps the stiffness matrix to be equipped with either the total variation diminishing property [1] or the maximum principle [22–24]. The monotonic solution profile, thus, results. Instead of modifying the test functions, Rice and Schnipke [20] and Hill and Baskharone [25] achieved the same goal by evaluating the convection terms along the local streamline. Recently, Ahue and Telias [24] used an exponential test function to construct an M-matrix. Inspired by their idea, we have constructed a weighting function which favors the field variable at the upstream side [26–29]. This upwind scheme and the mathematically rigorous theory of the

M-matrix constitute the building block for capturing sharp gradients or discontinuities in the flow.

In the following, we first describe in Section 2 the convection-diffusion model equation. This is followed by a brief introduction to two monotonicity-preserving finite element models. In our effort to obtain higher accuracy in the finite element model, we have made full use of the two underlying monotonic schemes and combined them linearly to achieve the goal without sacrificing stability. In order to validate the proposed flux discretization scheme, we consider in Section 3 a problem with a closed-form solution in a square cavity. In Section 4, two numerical examples are discussed, both of which have high-gradient solutions. Attention is given to assessing the chosen weighting factor α, which characterizes the accuracy, stability, and usefulness of the composite scheme proposed in this article. Some conclusions are given in the last section.

2. MULTI-DIMENSIONAL FINITE ELEMENT MODELS

2.1. *Model Equation*

As a working equation for the development of the finite element model, we consider in this paper the steady-state scalar equation. The model equation given below simulates the transport of a passive field variable Φ in a two-dimensional domain:

$$u\Phi_x + v\Phi_y = \mu(\Phi_{xx} + \Phi_{yy}). \tag{1}$$

For ease of illustration, we will restrict our attention to the case with $u = c_1$, $v = c_2$, where c_i $(i = 1, 2)$ are constant values. This constant flow assumption avoids invoking linearization of the equation. In what follows, μ is kept fixed in the simply connected domain D to simplify our presentation of the proposed scheme. Since we are examining the elliptic partial differential equation, we demand specification of Φ on the entire boundary of the physical domain D.

2.2. *Finite Element Model*

Our strategy for obtaining finite element solutions, $\hat{\Phi}$, to the transport Eq. (1) is to demand that the residual $R = u\hat{\Phi}_x + v\hat{\Phi}_y - \mu(\hat{\Phi}_{xx} + \hat{\Phi}_{yy})$ be orthogonal to the test space. The derivation is followed by substitution of bilinear basis functions, say N_i for $\hat{\Phi} = \sum_{i=1}^{4} N_i(\xi, \eta)\Phi_i$, into the weighted residuals statement to yield stiffness matrices for each element. This is followed by assemblage of elements and application of a frontal solver to obtain finite element solutions. In the development of the finite element model, it involves the selection of a test space to close the algebraic system. The choice of test (or weighting) functions is crucial to the search for the weak solutions to Eq. (1) when the maximum values of $Pe_x = \frac{u\Delta x}{\mu}$ and $Pe_y = \frac{v\Delta y}{\mu}$ greatly exceed the critical value of 2.

2.2.1. *Legendre polynomial finite element model.* The upwind finite element model is the method of choice to model the transport phenomena governed by Eq. (1). In our approach, stability is enhanced through specification of spatially unequal weights so that field variables at the upwind side are favored. To retain scheme consistency, application of biased weighting to diffusive fluxes is also needed. Use of bilinear basis functions to

approximate the scalar variable Φ presents another difficulty in the finite element analysis of Eq. (1). Difficulties arise from bilinear basis functions whose order is too low to render accurate numerical integration of diffusive terms. Also, the biased part of the test function which usually appears along with terms like $\frac{\partial N_i}{\partial x}$ or $\frac{\partial N_i}{\partial y}$ causes the accuracy to deteriorate. This suggests rational use of finite element spaces which permit infinite differentiation. It is for this reason that Sheu *et al.* [27] chose Legendre polynomials to span weighting functions. This is a desirable feature as it enhances convective stability for the model Eq. (1).

In a discretized domain with grid spacings h_ξ and h_η, our implementation involves use of weighting functions given by

$$W_i = D_i[d_{\xi_0} P_0(\xi) + d_{\xi_1} P_1(\xi)][d_{\eta_0} P_0(\eta) + d_{\eta_1} P_1(\eta)]. \tag{2}$$

Five coefficients are involved in the above equation which are given as

$$D_i = \frac{1}{4} \exp\left(\frac{u h_\xi \xi_i}{2\mu}\right) \exp\left(\frac{v h_\eta \eta_i}{2\mu}\right),$$

$$d_{\xi_n} = \frac{2n+1}{2} \int_{-1}^{1} W_\xi(t) P_n(t)\, dt,$$

$$d_{\eta_n} = \frac{2n+1}{2} \int_{-1}^{1} W_\eta(t) P_n(t)\, dt,$$

where

$$W_\xi(\xi) = (1 + \xi_i \xi) \exp\left(-\frac{u h_\xi \xi}{2\mu}\right),$$

$$W_\eta(\eta) = (1 + \eta_i \eta) \exp\left(-\frac{v h_\eta \eta}{2\mu}\right).$$

Specific to our implementation is the introduction to Legendre polynomials $P_0(t) = 1$ and $P_1(t) = t$ to the weighted residuals statement. Compared to our exponential finite element model [28], the computational efficiency is gained from the orthogonal property given as

$$\int_{-1}^{+1} P_i(t) P_j(t)\, dt = \frac{2}{2i+1} \delta_{i,j} \qquad (i \text{ is the dummy index}). \tag{3}$$

This is a desirable feature because a considerable amount of CPU time is saved in the calculation of integral terms. It is fair to conclude that the embedded orthogonal property makes the model presented here particularly appealing and motivates us to rewrite the bilinear shape functions $N_i(\xi, \eta)$ as functions of Legendre polynomials P_0 and P_1. For this study the shape functions are spanned by Legendre polynomials as

$$N_i(\xi, \eta) = \frac{1}{4}[P_0(\xi) + \xi_i P_1(\xi)][P_0(\eta) + \eta_i P_1(\eta)]. \tag{4}$$

According to the maximum principle, a real irreducible diagonally dominant matrix whose off-diagonal entries are non-positive is essential to obtain a monotonic solution profile. This suggests further investigation into whether the Legendre polynomial finite

element framework can truly yield an unconditionally monotonic solution. As in the finite difference method, we derive the representative equation for each node and assemble them into a compact form involving a nine-point stencil. The weighting coefficients are functions of Peclet numbers. By varying the values of P_{e_x} and P_{e_y}, we can determine whether or not the matrix equation is equipped with the sufficient (but not necessary) condition, without which monotonic solutions are impossible to compute. As this fundamental study reveals, computed solutions are, by definition, monotonic when Peclet numbers fall below 3.6 [28].

2.2.2. *Finite element model of Rice and Schnipke.* As said earlier in Subsection 2.2.1, use of the Legendre polynomial finite element model to solve Eq. (1) suffers from a restrictive stability condition. This is a drawback in the sense that monotonic solutions can be obtained only within a limited Peclet-number range. Too tight of a monotonicity leads to expensive solution costs because many refined grids are needed. There is therefore a strong need for a further refinement of the scheme. To this end, our strategy for improving computational efficiency is to extend the range of monotonic stability. In this study, we use the scheme of Rice and Schnipke [20] to extend the scope of application.

According to Rice and Schnipke [20], in each element the value of $u_s\Phi_s$ ($\equiv u\Phi_x + v\Phi_y$) is taken as a constant value. Following the standard finite element procedures, the elementary matrix equation, for the case of $u > 0$, $v > 0$, is obtained as

$$\begin{pmatrix} 0 & 0 & 0 & 0 \\ 0 & 0 & 0 & 0 \\ -F_pF_n\frac{u_s}{\Delta s}A_f & -(1-F_n)\frac{u_s}{\Delta s}A_f & \frac{u_s}{\Delta s}A_f & -(1-F_p)\frac{u_s}{\Delta s}A_f \\ 0 & 0 & 0 & 0 \end{pmatrix}. \tag{5}$$

For the notations involved in Eq. (5), they are defined as

$$A_f = \iint N_3(\xi,\eta)|J|\,d\xi\,d\eta, \tag{6a}$$

$$0 \le F_p \equiv \max\left\{\min\left(\frac{F_1}{F_2},1\right),0\right\} \le 1, \tag{6b}$$

$$0 \le F_n \equiv \max\left\{\min\left(\frac{F_4}{F_3},1\right),0\right\} \le 1, \tag{6c}$$

where

$$F_1 = v(-x_2+x_1) + u(y_2-y_1), \tag{6d}$$

$$F_2 = v(x_3-x_2) - u(y_3-y_2), \tag{6e}$$

$$F_3 = v(x_4-x_3) - u(y_4-y_3), \tag{6f}$$

$$F_4 = v(x_4+x_1) + u(y_1-y_4). \tag{6g}$$

As shown Fig. 1, Δs represents the length

$$\Delta s = \left((x_3-x')^2 + (y_3-y')^2\right)^{1/2}. \tag{7}$$

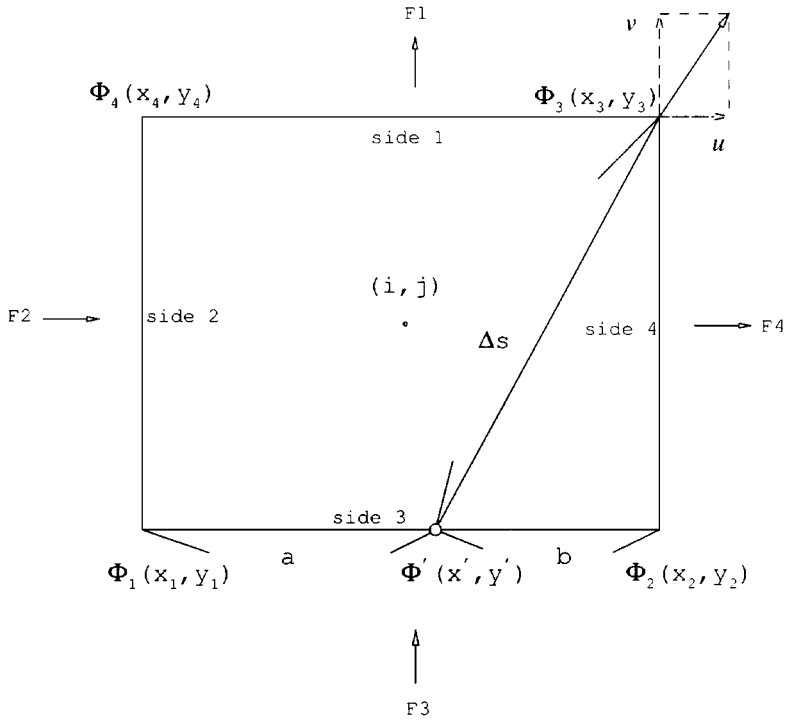

FIG. 1. An illustration of notations involved in the finite element model of Rice and Schnipke.

3. DEVELOPMENT OF A HIGH-RESOLUTION COMPOSITE SCHEME

As a first step towards better understanding of the finite element models presented in the previous section, we considered a problem that admits an analytic solution. The problem, as configured in Fig. 2, is subject to analytically prescribed boundary data. The exact solution

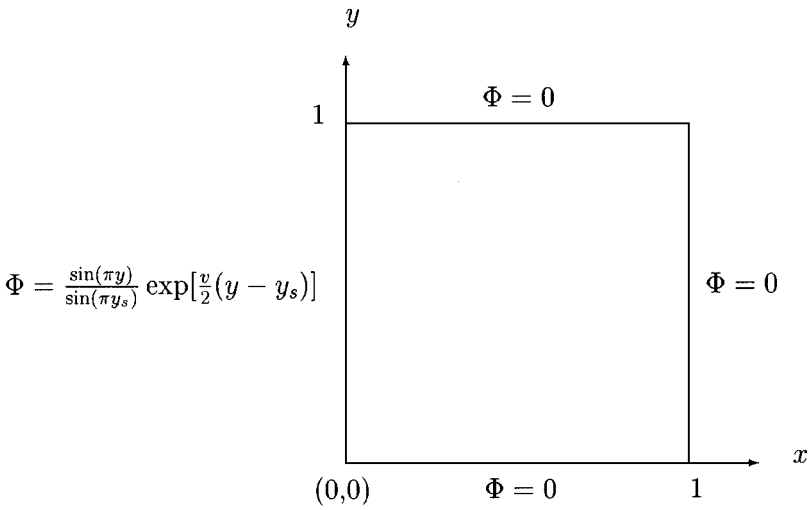

FIG. 2. An illustrative example used in the fundamental study of finite element models.

for the advection-diffusion Eq. (1) thus takes the boundary-layer form

$$\Phi(x, y) = \frac{\sin(\pi y)\exp(r_2 x)\exp[(v/2)(y - y_s)]\{1 - \exp[(r_1 - r_2)(x - 1)]\}}{[1 - \exp(r_2 - r_1)]\sin(\pi y_s)}, \quad (8)$$

where h is the grid size and

$$u = \frac{\mu}{4h}\cot\theta,$$
$$v = \frac{\mu}{4h},$$
$$\theta = \tan^{-1}\left(\frac{v}{u}\right),$$
$$y_s = 1 - \frac{1}{\pi}\tan^{-1}\left(\frac{2\pi}{v}\right),$$
$$r_1 = \frac{1}{2}\left[u + \sqrt{u^2 + v^2 + 4\pi^2}\right],$$
$$r_2 = \frac{1}{2}\left[u - \sqrt{u^2 + v^2 + 4\pi^2}\right].$$

In this case, Peclet numbers are functions of θ:

$$P_{e_x} = \frac{1}{4}\cot\theta,$$
$$P_{e_y} = \frac{1}{4}.$$

Computations were conducted in a unit square with continuous refinement of grids, resulting in uniform grids with resolutions of 11×11, 21×21, 31×31, 41×41, and 51×51. For this study, three different values of θ (15°, 2°, 1°) were considered. Clearly revealed by the computed L_2-error norms, as shown in Tables 1 and 2, is that the Legendre polynomial finite element model is the method of choice for problems with lower Peclet numbers while for cases with higher Peclet numbers, it is preferable to use the characteristic Galerkin finite element model. Revealed also by this study is that oscillatory solutions are never found in the characteristic finite element model. The Legendre polynomial finite element model, on the other hand, outperforms the characteristic model in view of the improving prediction accuracy. These tests support the idea of blending the two techniques together in the hope

TABLE 1
Computed L_2-Error Norms for the Problem Defined in Section 3 Using the Legendre Polynomial Finite Element Model

Grid	$\theta = 15^\circ$ ($P_{e_x} = 0.933$)
11×11	2.125×10^{-3}
21×21	1.660×10^{-3}
31×31	8.979×10^{-4}
41×41	4.763×10^{-4}
51×51	3.040×10^{-4}

TABLE 2
Computed L_2-Error Norms at Different Values of θ for the Problem, Defined in Section 3, Using the Characteristic Galerkin Finite Element Model

Grid	$\theta = 15^\circ$ ($P_{e_x} = 0.933$)	$\theta = 2^\circ$ ($P_{e_x} = 7.159$)	$\theta = 1^\circ$ ($P_{e_x} = 14.322$)
11×11	1.368×10^{-1}	1.420×10^{-1}	9.212×10^{-2}
21×21	1.541×10^{-1}	9.768×10^{-2}	5.905×10^{-2}
31×31	1.414×10^{-1}	8.614×10^{-2}	5.331×10^{-2}
41×41	1.267×10^{-1}	8.165×10^{-2}	5.147×10^{-2}
51×51	1.133×10^{-1}	7.843×10^{-2}	4.990×10^{-2}

of extending the range of application while still minimizing the oscillations and, in turn, the prediction errors. In this way, we suggest

$$A = (1 - \alpha)A|_{Legendre\text{-}polynomial} + \alpha A|_{characteristic\ Galerkin}. \tag{9}$$

In still remains to determine the weighting coefficient α in Eq. (9). Our strategy to specify the value of α is that each 4×4 stiffness matrix is maintained as an M-matrix. In each i-row of the matrix equation, α_i is chosen in a way that the matrix equation is of the M-matrix type. The assembled finite element matrix equation is, thus, classified as an M-matrix. The justification for using our composite scheme is clearly seen in Fig. 3 which plots the computed finite element solutions. There exist oscillations near the jump when using the Legendre polynomial finite element model. As Table 3 shows, the composite method presented here outperforms the model of Rice and Schnipke in the sense that the accuracy is improved while stability is still well maintained. Also shown from Fig. 3 is that the method presented in this article improves the stability while it maintains the accuracy, as compared with solutions computed using the Legendre polynomial finite element model.

4. NUMERICAL RESULTS

4.1. *Skew Advection-Diffusion Problem*

The first problem considered in this section is known as the skew flow transport problem which is regarded as a worst case scenario for assessing upwinding methods. This problem is configured in Fig. 4. What is most apparent in this figure is that there is a tilted line which passes through a corner point at (0, 0), resulting in a line with a slope of $m = v/u$.

TABLE 3
Computed L_2-Error Norms at Different Values of θ for the Problem, Defined in Section 3, Using the Composite Finite Element Model

Grid	$\theta = 15^\circ$ ($P_{e_x} = 0.933$)	$\theta = 2^\circ$ ($P_{e_x} = 7.159$)	$\theta = 1^\circ$ ($P_{e_x} = 14.322$)
11×11	2.125×10^{-3}	7.522×10^{-2}	5.800×10^{-2}
21×21	1.660×10^{-3}	5.132×10^{-2}	3.977×10^{-2}
31×31	8.976×10^{-4}	4.694×10^{-2}	3.703×10^{-2}
41×41	4.757×10^{-4}	4.507×10^{-2}	3.589×10^{-2}
51×51	3.036×10^{-4}	4.332×10^{-2}	3.465×10^{-2}

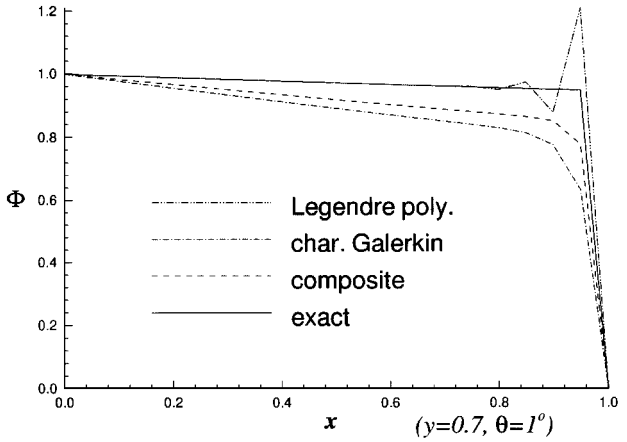

(a)

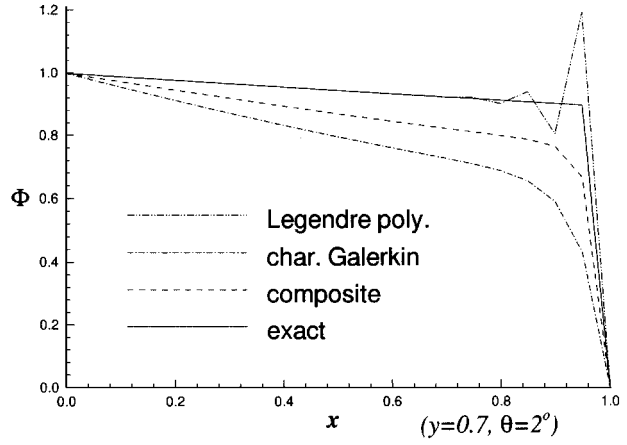

(b)

FIG. 3. Computed solutions of $\Phi(x, y = 0.7)$ in a grid with the resolution of 21×21. (a) Solutions were computed for the case of $\theta = 1^\circ$; (b) solutions were computed for the case of $\theta = 2^\circ$; (c) solutions were computed for the case of $\theta = 15^\circ$.

Inside the unit square cavity the y-component velocity is invariant with a fixed value of $v = 1$. According to the boundary data prescribed in Fig. 4, there is a marked change of the solution across the dividing line.

The aim of investigating this case is to show the effectiveness of applying the proposed composite monotonic scheme to resolve high-gradient solutions in the flow. Tests were carried out in a unit square covered with grids of different resolutions, and for fluids with different diffusivities. As Fig. 5 shows, solution profiles $\Phi(x, y = 0.5)$ were well captured without showing oscillatory behavior.

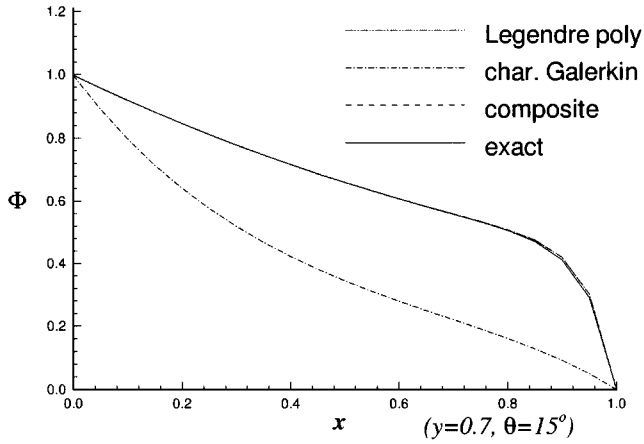

(c)

FIG. 3—*Continued*

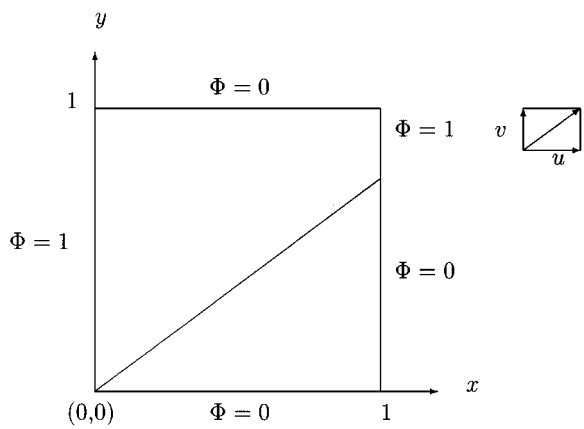

FIG. 4. An illustration of the skew advection-diffusion test problem considered in Subsection 4.1.

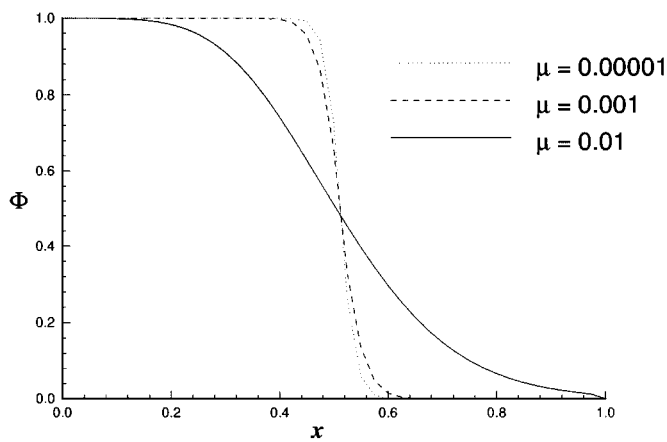

FIG. 5. Plot of Φ at $y = 0.5$ for grids with different resolutions and for fluids with different diffusivities using the composite finite element model.

TABLE 4
Computed L_2-Error Norms Using Different Schemes for the Problem Considered in Subsection 4.2

Grid	Composite	Rate of convergence	Char. Galerkin	Rate of convergence
11×11	3.385		8.973	
21×21	5.585×10^{-1}	2.60	4.328	1.05
31×31	1.289×10^{-1}	3.62	2.801	1.07
41×41	3.418×10^{-2}	4.61	2.083	1.03
51×51	9.902×10^{-3}	5.55	1.679	0.96

4.2. *A Variable Advection-Diffusion Problem*

We close this section with the test case involving variable advective velocities. Such an effort is worthwhile to justify the applicability of this composite model to simulate realistic flow problems. For this study, the velocity components under investigation are given by

$$u = -2\lambda\nu \tanh[\lambda(x - x_0)], \tag{10a}$$

$$v = a_1 \tan(a_2 y). \tag{10b}$$

Given these variable velocities, the exact solution to Eq. (1) takes the form exactly the same as u shown in Eq. (10a). The case considered was that of $x_0 = 1$, $\lambda = 100$, $a_1 = 50$, $a_2 = 1.5$. Depending on the assigned value of ν (=1 for the present case), the analytic solution of Φ can show different degrees of internal gradients. In the test, we constructed element matrix equations from two different models and summed them according to the weighting factor α plotted in Fig. 6. As Figs. 7, 8 and Table 4 show, we can clearly see the advantage of using a composite scheme in stability as well as in accuracy.

5. CONCLUDING REMARKS

We have presented in this paper a composite scheme for solving the scalar advection-diffusion equation in two dimensions. For this study, two classes of monotonic finite element schemes were selected for use as contributing schemes. The discrete maximum principle served as the underlying guideline for judging whether or not solution monotonicity could be achieved. The first model employs the Legendre polynomial to span the finite element space. This model is application infeasible because this scheme is classified as monotonic only when the Peclet number falls below 3.6. The other approach considered here is due to Rice and Schnipke. Chief among the reasons for this choice is that this scheme has the M-matrix property in all ranges of Peclet numbers. A potential drawback of this scheme is that this approach is less accurate in the case of lower Peclet numbers. In the light of the above observations we take the model of Rice and Schnipke as an cure for the stability improvement using the Legendre polynomial model. The key to constructing this scheme is to properly select the weighting factor. Some insight into the selection of α has been gained by performing a fundamental study in an attempt to maintain higher solution accuracy but not at the loss of scheme stability.

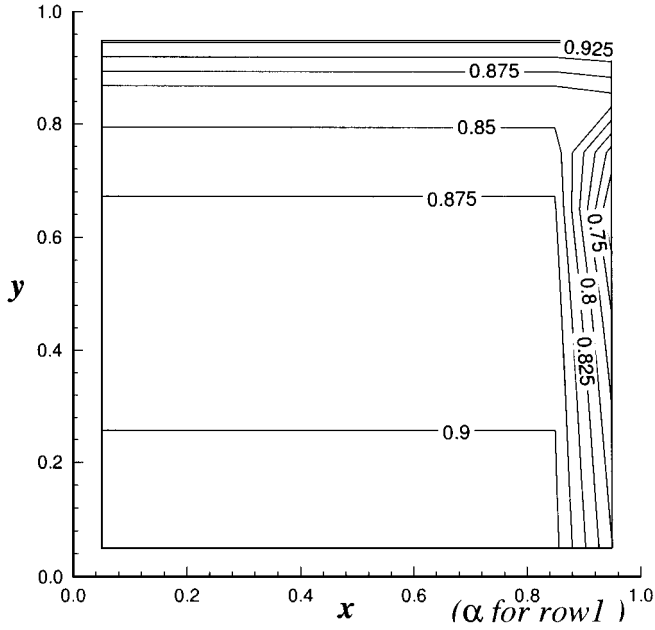

(a)

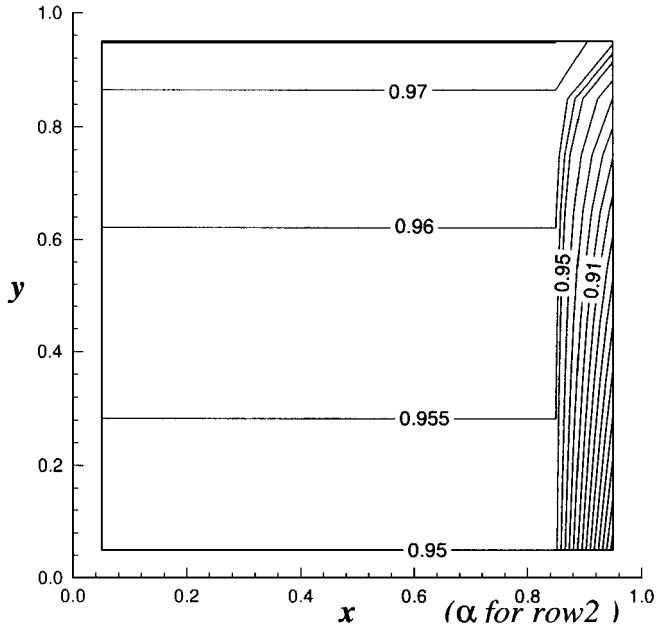

(b)

FIG. 6. A contour map of α, as defined in (9), for the problem defined in Subsection 4.2. (a) Distribution for the first row of each element; (b) distribution for the second row of each element; (c) distribution for the third row of each element; (d) distribution for the fourth row of each element.

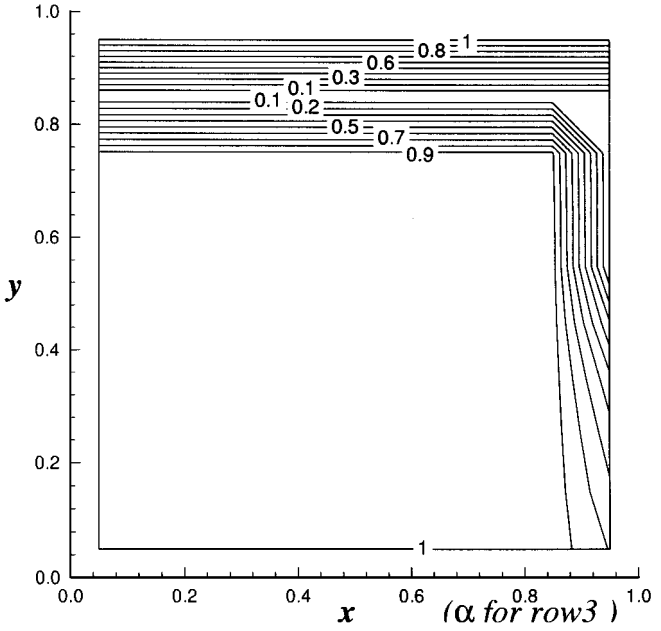

(c)

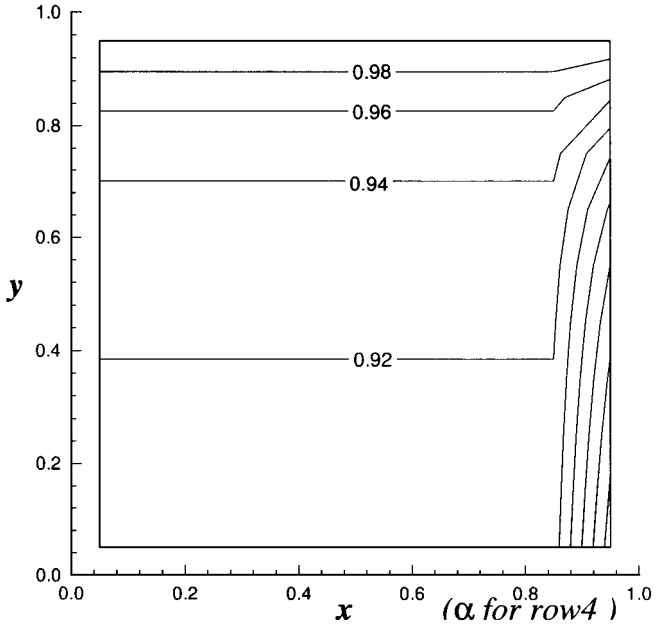

(d)

FIG. 6—*Continued*

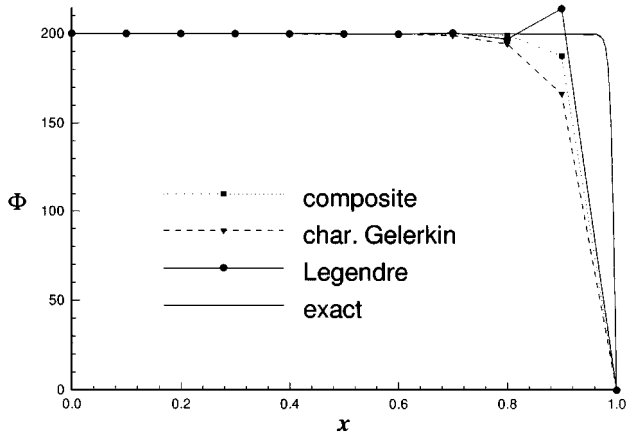

(a)

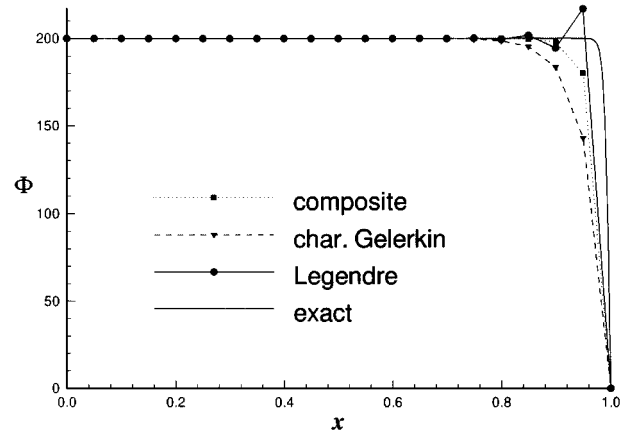

(b)

FIG. 7. Computed solutions of $\Phi(x, y = 0.5)$ using different finite element models. (a) Solutions were computed at 11×11 grids; (b) solutions were computed at 21×21 grids.

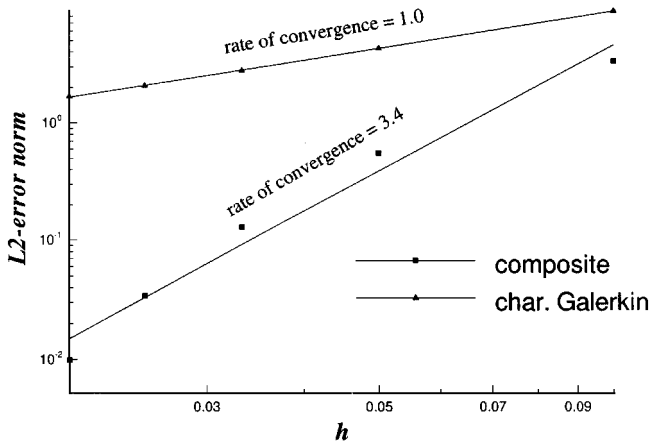

FIG. 8. Rates of convergence for the problem considered in Subsection 4.2.

ACKNOWLEDGMENTS

The authors thank the Computer Center of National Taiwan University and the National Center for High-performance Computing (NCHC) for providing CRAY J916 and IBM RS/6000-590 computers, which made this study possible. Research support by the National Science Council under Grant NSC84-2212-E-002-060 is also gratefully acknowledged.

REFERENCES

1. A. Harten, High resolution schemes for hyperbolic conservation law, *J. Comput. Phys.* **49**, 357 (1983).
2. J. P. Boris and D. L. Book, Flux corrected transport. I. SHASTA, a fluid transport algorithm that works, *J. Comput. Phys.* **11**, 38 (1973).
3. S. T. Zalesak, Fully multidimensional flux-corrected transport algorithm for fluids, *J. Comput. Phys.* **31**, 335 (1979).
4. P. Woodward and P. Colella, The numerical simulation of two-dimensional fluid flow with strong shocks, *J. Comput. Phys.* **54**, 115 (1984).
5. M. Chapman, FRAM-nonlinear damping algorithm for the continuity equation, *J. Comput. Phys.* **44**, 84 (1981).
6. P. K. Sweby, High resolution schemes using flux limiters for hyperbolic conservation laws, *SIAM J. Numer. Anal.* **121**, 995 (1984).
7. T. W. H. Sheu, S. M. Lee, K. O. Yang, and B. J. Y. Chiou, A non-oscillating solution technique for skew and QUICK-family schemes, *Comput. Mech.* **8**, 365 (1991).
8. B. P. Leonard, Simple high-accuracy resolution program of convective modeling of discontinuity, *Int. J. Numer. Methods Fluids* **8**, 1291 (1988).
9. B. P. Leonard, A. P. Lock, and M. K. MacVean, The NIRVANA scheme applied to one-dimensional advection, *Int. J. Numer. Methods Heat Fluid Flow* **5**, 341 (1995).
10. B. P. Leonard, A. P. Lock, and M. K. MacVean, Extend numerical integration for genuinely multidimensional advective transport insuring conservation, *Numer. Methods Laminar Turbulent Flow* **9**(1), 1 (1995).
11. P. H. Gaskell and A. K. C. Lau, Curvature compensated convective transport: SMART a new boundedness preserving transport algorithm, *Int. J. Numer. Methods Fluids* **8**, 617 (1988).
12. R. Lönher, K. Morgan, J. Peraire, and M. Vahdati, Finite element flux-corrected transport (FEM-FCT) for the Euler and Navier-Stokes equations, *Int. J. Numer. Methods Fluids* **7**, 1093 (1987).
13. T. W. H. Sheu and C. C. Fang, A high resolution finite element analysis for nonlinear acoustic wave propagation, *J. Comput. Acoustics* **2**, 29 (1994).
14. T. W. H. Sheu and C. C. Fang, A numerical study of nonlinear propagation of disturbances in two-dimensions, *J. Comput. Acoustics* **4**(3), 291 (1996).
15. T. W. H. Sheu and C. C. Fang, A flux corrected transport finite element method for multi-dimensional gas dynamics, in *Proceedings, Second European Computational Fluid Dynamics Conference (ECCOMAS), 1994*, p. 170.
16. H. Deconinck, H. Paillére, R. Struijs, and P. L. Roe, Multidimensional upwind schemes based on fluctuation-splitting for systems of conservation laws, *J. Comput. Mech.* **11**, 323 (1993).
17. A. C. Galeão and E. G. Dutra do Carmo, A consistent approximate upwind Petrov-Galerkin formulation for convection-dominated problems, *J. Comput. Methods Appl. Mech. Eng.* **68**, 83 (1988).
18. A. N. Brooks and T. T. R. Hughes, Streamline upwind Petrov-Galerkin formulations for convection-dominated flows with particular emphasis on the incompressible Navier-Stokes equations, *J. Comput. Methods Appl. Mech. Eng.* **32**, 199 (1982).
19. S. Spekreijse, Multigrid solution of monotone second-order discretizations of hyperbolic conservation laws, *Math. Comp.* **49**, 135 (1987).
20. J. G. Rice and R. J. Schnipke, A monotone streamline upwind finite element method for convection-dominated flows, *Comput. Methods Appl. Mech. Eng.* **47**, 313 (1983).

21. T. W. H. Sheu, P. G. Y. Huang, and M. M. T. Wang, A discontinuity SUPG formulation using quadratic elements, in *Proceeding, First European Computational Fluid Dynamics Conf., 1992* (edited by Ch. Hirsch), Vol. 1, p. 125.
22. T. Meis and U. Marcowitz, Numerical solution of partial differential equations, in *Applied Mathematical Science* (Springer-Verlag, New York/Berlin, 1981), Vol. 32.
23. T. Ikeda, Maximal principle in finite element models for convection-diffusion phenomena, in *Numerical and Applied Analysis* (North-Holland, Kinokuniya/Amsterdam, 1983), Vol. 4.
24. M. Ahue and M. Telias, Petrov-Galerkin scheme for the steady state convection diffusion equation, *Finite Elements Water Resources* **2**/**3** (1982).
25. D. L. Hill and E. A. Baskharone, A monotone streamline upwind method for quadratic finite elements, *Int. J. Numer. Methods Fluids* **17**, 463 (1983).
26. T. W. H. Sheu, M. M. T. Wang, and S. F. Tsai, A Petrov-Galerkin finite element model for analyzing incompressible flows at high Reynolds numbers, *Int. J. Comput. Fluid Dynam.* **5**, 213 (1995).
27. T. W. H. Sheu, S. F. Tsai, and M. M. T. Wang, A monotone multi-dimensional upwind finite element method for advection-diffusion problems, *Numer. Heat Transfer Part B Fundamentals* **29**, 325 (1996).
28. T. W. H. Sheu, S. F. Tsai, and M. M. T. Wang, A monotone finite element method with test space of Legendre polynomials, *Comput. Methods Appl. Mech. Eng.* **143**, 349 (1997).
29. T. W. H. Sheu, S. F. Tsai, and M. M. T. Wang, Monotonic multi-dimensional flux discretization scheme for all peclet numbers, *Numer. Heat Transfer Part B Fundamentals* **31**, 441 (1997).